

Jarosław Janicki,  
Marcin Bączek

# Supramolecular Structure and Properties of PA6-LCO Molecular Composite Fibres

Institute of Textile Engineering  
and Polymer Materials,  
University of Bielsko-Biala,  
43-309 Bielsko-Biala, Willowa 2, Poland  
E-mail: jjanicki@ath.bielsko.pl  
mbaczek@ath.bielsko.pl

## Abstract

Nowadays polyamides have become essential in fibre production for textiles and technical uses. However, such applications require extremely high strength parameters as well as excellent dimensional stability. In order to improve polymer properties they are reinforced with glass fibres or with very high strength and high modulus liquid crystalline polymers. In this work fibres formed from a new category of high-performance polymeric materials, called molecular composites, were studied with a focus on the effect of liquid crystalline oligoester on the structure of thermoplastic polymer matrix. The supramolecular structure of the fibres was characterised by the wide and small angle x-ray scattering (WAXS and SAXS) techniques while the Differential Scanning Calorimetry (DSC) method was used for thermal characterisation. In addition some mechanical parameters of undrawn fibres are presented.

**Key words:** supramolecular structure, supramolecular properties, polyamide 6, liquid crystalline polymer, WAXS, SAXS, DSC.

This work is focused on the influence of LCO on the supramolecular structure of the fibres prepared from the new LCP and polyamide 6 (PA6) blends. The WAXD technique is used to characterise crystalline polymorphs, crystallite size and crystallinity of the polymer matrix of fibres, while parameters of the lamellar structure are extracted from the SAXS patterns. Thermal properties are discussed in the context of Differential Scanning Calorimetry (DSC) results, and some results of the mechanical tests are presented as well. The morphological parameters of non-modified PA6 fibres are included for comparison.

ing, extrusion, and annealing at temperature above  $T_m$  of LCO and below  $T_m$  of polymer.

## Formation of fibres

Fibres from PA6-LCO molecular composites were formed using a prototype single-head laboratory extruder. An extruder's head consists of a spinneret with a single hole of diameter  $\phi = 0,2\text{mm}$ . Nanocomposites were melted in a mass cylinder and extruded under a pressure of 0.5 MPa. During the formation process the temperature of the spinneret was set at 240 °C. The fibres were spun with a take-up velocity of 26 m/min.

## Introduction

Polyamides have become essential materials in fibre production for textiles and technical uses. However, such applications require extremely high strength parameters as well as excellent dimensional stability. In order to improve polymer properties they are reinforced with glass fibres or with very high strength and high modulus liquid crystalline polymers (LCP). The blending of thermotropic LCP with semicrystalline thermoplastic polymers to form in-situ polymer composites is of great advantage because of the lowered viscosity during processing. Furthermore, LCP act as reinforcing elements in the blend and its addition to a polymer matrix has a profound impact on the physical and mechanical properties of the final product. However, the melting temperature of liquid crystalline polymers is usually too high for processing semicrystalline thermoplastic polymers. In order to reduce the melting and transition temperature, a new LCP, with flexible units in the main chain, were synthesised [1].

## Experimental

### Materials

A molecular composite for fibre formation was prepared from PA6 and liquid crystalline oligoester (LCO) with 90% of PA6 and 10% of LCO by weight. The LCO were provided by the "Centre of Polymer and Carbon Research of the Polish Academy of Science, Zabrze". In the molecular structure of LCO, aromatic rings of the mesogen are bonded with ester groups, while the aliphatic end-groups consisting of eleven carbon atoms, are connected to the aromatic ring by ester bonds, as shown in Figure 1. The preparation of the molecular composites consists of three essential stages: blend-

## Analytical methods

### WAXS

Static WAXS measurements at room temperature of powdered fibres were performed at room temperature on a URD 6 Seifert diffractometer operated at 40 kV and 30 mA. Incident x-rays from a copper target sealed tube were monochromatised using a Ni filter. Scattered radiation with a wavelength  $\lambda_{\text{CuK}\alpha} = 0.15418\text{ nm}$  was detected by a scintillation counter over an angular range of 5 and 60° of  $2\theta$  and at a step scan size of 0.1. Experimental diffraction patterns were corrected for the polarisation and Lorentz factor. After the subtraction of incoherent scattering

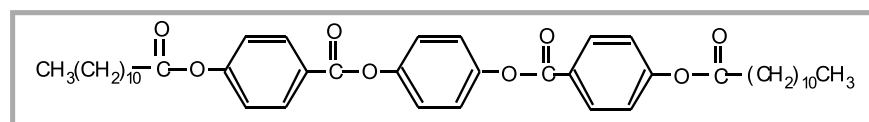


**Figure 1.** The macromolecular chain of liquid crystalline oligoester used as a component of PA6-LCO molecular composite.

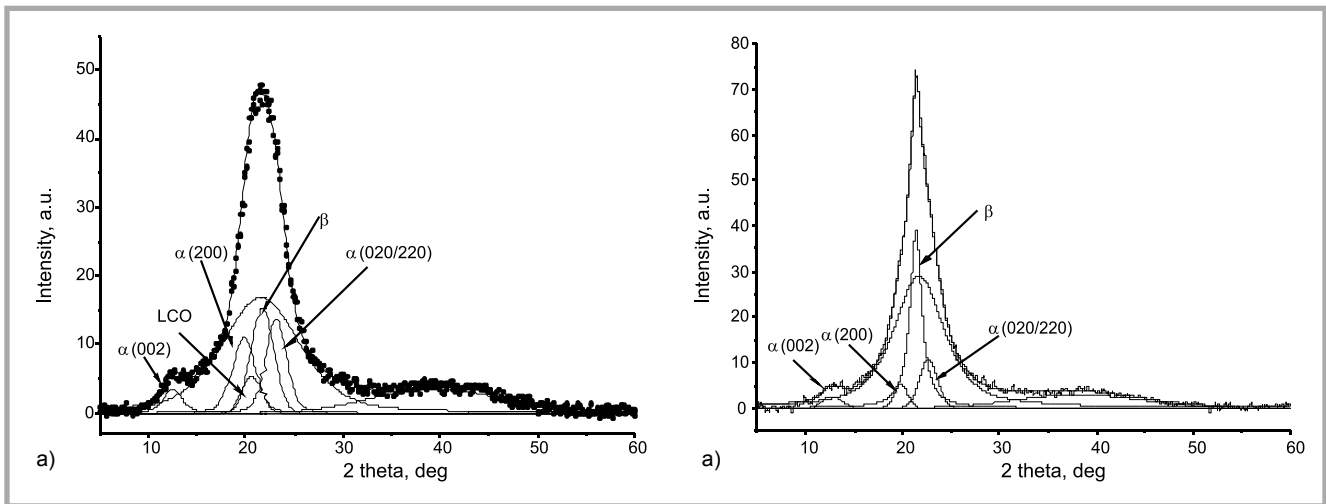


**Figure 2.** WAXS curves resolved for individual peaks. Marked diffraction reflexes with adequate Miller indices: a) curve for PA6-LCO fibre, b) curve for PA6 fibre.

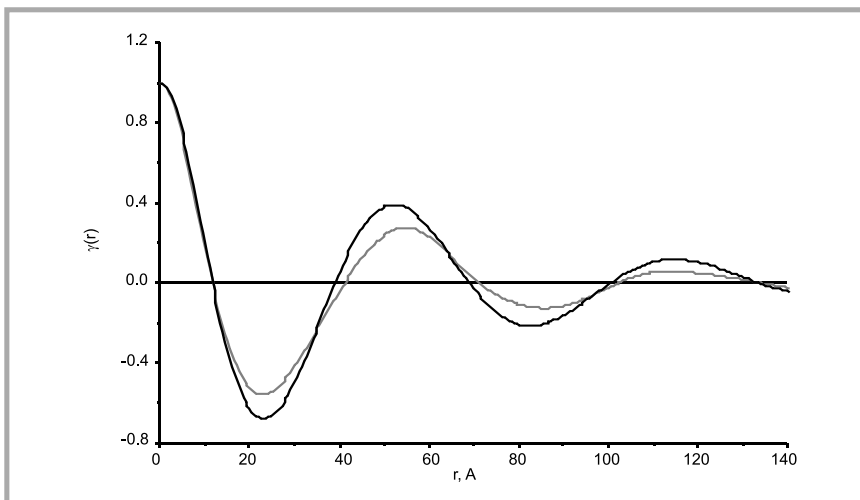


**Figure 3.** Correlation functions calculated from SAXS data for PA6 (black) and PA6-LCO (grey) fibres.

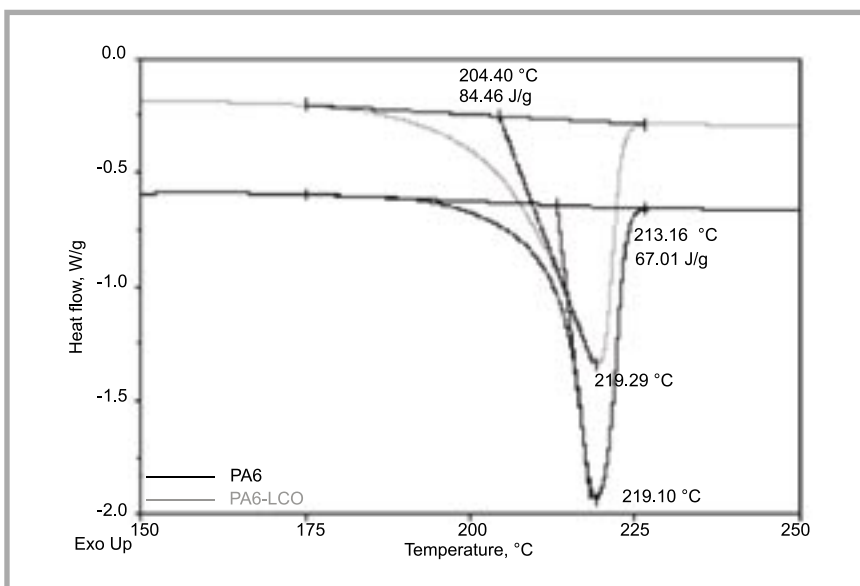


**Figure 4.** DSC thermograms in the polyamide melting area for PA6-LCO (grey) and PA6 (black) fibres. Characteristic temperatures and the enthalpy of phase transition are determined.

and linear background, the curves were decomposed into a crystalline reflection and amorphous halo using WAXSFIT software [3]. The fraction of the crystalline phase was calculated from the ratio of the area under the crystalline reflections and the total WAXS intensity. The lateral dimension of the crystallites in the direction perpendicular to the planes was estimated from the full width at half maximum of the corresponding crystalline peak using Scherrer's equation [4]. In the case of PA6-LCO fibres, the LCO peak was taken into consideration.

### SAXS

Small-angle X-ray scattering patterns were recorded with a MBraun SWAX camera with a Kratky collimation system, equipped with a PSD 50 MBraun linear position sensitive detector. The X-ray tube was a conventional copper anode operated at 40 kV and 30 mA controlled by a Philips PW 1830 x-ray generator. Cu  $K_{\alpha}$  radiation was obtained by filtering with Ni and pulse height discrimination. The powders were measured at room temperature while being kept in a standard sample holder, sealed with aluminium foils. A blank scattering was subtracted taking sample transmission into account. The experimental SAXS curves were de-smearred from collimation distortion by means of a 3DVIEW MBraun computer program. Normalised correlation functions were calculated as a function of  $r$ , the distance in real space, according to the procedure described in [5].

### DSC

DSC data were collected using a 2920 DSC type of the 5100 Instruments Ther-

mal Analysis System. The samples were heated at 10 °C/min (atmosphere N<sub>2</sub>; flow 40 ml/min) in a wide temperature range (-40 – 290 °C). The heat and temperatures of the transitions were calculated using Universal V2.6D TA Instruments software. The onset of the transition ( $T_{ON\ SET}$ ) was determined by a standard method as the intersection point tangent to the front of the heat at the point of inflection with the baseline [2]. Based on the DSC measurements, the mass crystallinity of fibres was calculated according to the following equation:

$$\kappa = \frac{\Delta H_m}{\Delta H_{100}} \quad (1)$$

where  $\Delta H_m$  is the measured value of the melting enthalpy of fibre,  $\Delta H_{100}$  is the enthalpy of 100% crystalline PA6 [6].

### Mechanical tests

Tensile strength parameters of the undrawn fibres were obtained by means of a INSTRON 5544 Single Column tensile testing machine, connected to a computer equipped with MERLIN software. The machine consists of a press-stretching head for fibres of static load cell rating  $\pm 10$  N with indication error 0.05%. Measurements were taken in normal climatic conditions for samples of 10 mm length. The tensile speed was 30 mm·min<sup>-1</sup> and 20 tests were made for each sample. On the basis of the measurements taken, we defined the breaking tenacity as well as the breaking elongation and modulus of elasticity.

### Results and discussion

The crystalline polymorphism of the fibres was identified on the basis of their WAXD patterns.

The WAXS data shown in Figure 2 reveal that both PA6 and PA6-LCO fibres exhibit polymorphism:  $\alpha$ -monoclinic form and  $\beta$ -hexagonal form co-exist. Table 1 presents the output of the WAXS and SAXS curves analysis. An addition of LCO to the polymer matrix causes 4% increase in crystallinity. On the other hand, the crystallite size gets smaller as compared to unmodified PA6 fibres; however, the differences are small.

The basic parameter of the lamellar structure developed during fibres formation is the long period,  $L$ , read from the first side maximum of the correlation function. Other structural parameters

**Table 1.** Results of WAXS and SAXS studies.

sample	crystallinity, %	$D_{\alpha}$ (200), nm	$D_{\alpha}$ (020/220), nm	$D_{\beta}$ , nm	$D_{\alpha}$ (002), nm	$L$ , nm	$lc$ , nm
PA6-LCO	34	3.3	3.5	3.4	3.6	5.5	1.7
PA6	30	6.0	4.3	5.7	3.7	5.2	1.8

**Table 2.** Selected tensile strength parameters of undrawn PA6 and PA6-LCO fibres.

sample	breaking tenacities, cN/tex	breaking elongation, %	modulus, cN/tex
PA6-LCO	6.9	770	0.40
PA6	10.5	600	0.16

like the crystalline lamellae, ( $lc$ ), and the thickness of the amorphous layer, ( $la$ ), were also calculated on the basis of the correlation function, since  $L = lc + la$ . The results are included in Table 1.

The correlation functions calculated from SAXS data of PA6 and PA6-LCO fibres are presented in Figure 3.

The comparison of DSC curves in the range of the melting area (Figure 4) shows the difference in the values of enthalpy in the transition phase  $\Delta H_m$  and the difference in the onset of the transition. On the other hand, the melting points,  $T_m$  of both of the fibres studied are almost the same.

The increase in enthalpy for PA6-LCO fibre is parallel to the increase in the degree of supermolecular structure arrangement, while the change in the shape of the melting peak, with lower  $T_{mON-SET}$  value may suggest an increase in the dispersion of crystallite dimensions.

The results obtained indicate that the presence of liquid crystalline oligoester causes an increase in the mass degree of the crystallinity of polymer matrix in PA6-LCO fibres (from 29% to 41%). However these results differ considerably from the WAXS results and are considered as approximate values, caused by an energetic contribution of temperature transformation between polymorphic phases (on thermograms we observed the additivity of enthalpy of temperature transformation between phases and the enthalpy of melting of the total crystalline phase in the samples).

Table 2 summarizes the results of the mechanical test. The presence of LCO has an influence on the mechanical parameters of fibres. A comparison analysis of the tensile curves shows that the breaking tenacity for PA6-LCO fibres

decreases while elongation at break increases, compared to the non-modified PA6 fibres. High modulus, high proof of stress and wide range of elasticity are characteristic of undrawn fibres from PA6-LCO molecular composites.

### Conclusions

Analysis of the supramolecular structure of fibres produced from PA6-LCO molecular composite shows, that liquid crystalline oligoester significantly influences the structure of polymer matrix in fibres. LCO is homogeneously dispersed at a molecular scale in thermoplastic PA6 polymer matrix. For this reason most of the parameters of fibre structure and their thermal and mechanical properties are changed. However, an exact determination of the quality, as well as the direction of these changes, proved to be a rather difficult task.

### References

1. Janicki J., *Nanostruktura i właściwości termiczne wybranych materiałów polimerowych (rozprawa habilitacyjna)*, Bielsko-Biała 2002.
2. Turi E.A., *Thermal Characterization of Polymeric Materials, Second Edition, Volume 1*, Academic Press, Brooklyn, New York 1997.
3. Rabiej M., Rabiej S., *Analiza rentgenowskich krzywych dyfrakcyjnych polimerów za pomocą programu WAXSFIT*, Wydawnictwo ATH, Bielsko Biała 2006.
4. Alexander L. E., *X-ray Diffraction Methods in Polymer Science*, Wiley, New York 1969.
5. Vonk C. G., Kortleve G., *Kolloid – Z. Z. Polymer*, 220, 19, (1967).
6. ATHAS databank <http://athas.prz.edu.pl>

Received 15.11.2007 Reviewed 15.01.2008